# The Importance of Site-Specific Seismic Nonlinear Ground Analysis in Eastern Canada

Zi Jing Zhang, Samuel Yniesta
*Department of Civil, Geological and Mining Engineering – Polytechnique Montreal, Montreal, Quebec, Canada*
Alain Plaisant
*Modeling and Soil Structure Interaction Department, WSP, Montréal, Québec, Canada*

ABSTRACT
In the current state of practice in Eastern Canada, the seismic hazard at a site is defined by the Geological Survey of Canada with a uniform hazard spectrum (UHS) for a site of class C, and modified using the site amplification factors recommended by the National Building Code of 2015 (NBCC 2015) or the Canadian Highway Bridge Design Code (S6-19). When necessary, site-specific ground response analysis are performed using equivalent linear ground response analysis, which considers an unrealistic assumption of constant dynamic properties during wave propagation. In this study, for a wide variety of soil sites in Quebec, dynamic simulations were conducted using the software DEEPSOIL to compute site-specific soil amplification factors. The site amplification factors from the NBCC 2015 and those computed using nonlinear 1D ground response analysis are then compared, and the results indicate larger amplification of the earthquake response spectrum around the site's natural period (or at periods slightly longer than the natural period) than the one calculated with the NBCC 2015 recommendations. Therefore, the NBCC 2015 may not always be conservative and could underestimate the seismic demand at a site.

RÉSUMÉ
Dans l'état actuel de la pratique dans l'est du Canada, l'aléa sismique d'un site est défini par la Commission Géologique du Canada par un spectre à l'aléa uniforme pour un site de classe C, puis modifié en utilisant les facteurs d'amplification recommandés par le Code national du bâtiment de 2015 (NBCC 2015) ou le code canadien sur le calcul des ponts routiers. Lorsque nécessaire, des analyses de réponse de dépôt spécifiques aux sites sont effectuées en utilisant une analyse équivalente linéaire, qui considère l'hypothèse irréaliste que les propriétés dynamiques sont constantes pendant la propagation des ondes. Dans cette étude, pour un grand nombre de sites au Québec, des analyses non-linéaires ont été réalisées à l'aide du logiciel DEEPSOIL pour calculer les facteurs d'amplification des sols spécifiques aux sites. Les facteurs d'amplification du NBCC 2015 et ceux calculés à l'aide des analyses 1D de réponse de site non-linéaires sont ensuite comparés, et les résultats suggèrent que les facteurs d'amplification du sol sont souvent plus élevés près de la période naturelle du site, ou à des périodes légèrement plus longues que la période naturelle, comparés aux recommandations du NBCC 2015. En conclusion, le NBCC 2015 n'est pas n'est pas toujours sécuritaire, et peut mener à sous-estimer la demande sismique à un site.

## 1. INTRODUCTION

When soft soil deposits overlay bedrock, seismic waves propagated from the bedrock are typically altered due to the impedance contrast between rock and soil. Soil effects can cause an amplification of the ground motion at the ground surface (Buech et al., 2010), or an attenuation, depending on the stiffness of the system, the nonlinearity of the soil, the frequency content and the intensity of the input motion. Among Canadian industry practices, the National Building Code of Canada 2015 (NBCC 2015) and the Canadian Highway Bridge Design Code 2019 (S6-19) offer a simple approach to determine soil effects, based on Borcherdt (1994), consisting of applying an amplification factor to the spectral acceleration at the bedrock based on the soil type determined by the average shear wave velocity of the first 30 meters below the surface or the foundation level ($V_{s30}$). This method relies on non-site specific empirical factors, that do not consider effects such as the duration of the motion, or its frequency content and are associated with significant uncertainty (Finn and Wightman 2003). In the NBCC 2005 and 2010, these factors were derived based on limited recordings from the Loma Prieta earthquake and ground response simulations (Finn and Wightman 2003), while the latest version of the Canadian building code uses factors derived from the Boore and Atkinson (2008) ground motion model. However, the latter were derived from a ground motion database that only included few recordings at soft sites, and its use is not recommended for $V_{S30}$ < 180 m/s. To overcome the limitations of such factors, the NBCC 2015 allows to perform site-specific site response analysis, in order to assess the amplification at a site. In fact, for site class F, such as liquefiable soils or sensitive clays, it is required to perform site-specific analysis.

One commonly used method to perform site-specific 1D ground response analysis (GRA) is the equivalent linear method, whose one-dimensional differential equation of wave propagation is solved in the frequency domain (Seed et Idriss, 1969, Schnabel et al., 1972). During an equivalent linear analysis, constant values of the soil modulus reduction and damping (MRD) are used. These values are adjusted iteratively in order to be consistent with the input MRD curves and the maximum strain computed throughout the deformation process. This method is not recommended due to the large source of error introduced to the results from the lack of consideration for the time-dependent dynamic properties, and the limitations of the aforementioned assumption. In contrast, the nonlinear method is a more rigorous approach which solves the equation of seismic wave propagation in the time domain, while considering the nonlinearity of the soil's cyclical behaviour (Kaklamanos et al., 2015) through a constitutive model. Multiple viable resources are available to adequately perform nonlinear analyses, such as the software DEEPSOIL (Hashash et al. 2017).

Historically, seismic demands and liquefaction potential were rarely a concern in Eastern Canada. The recent advances in the evaluation of seismic hazard in Eastern Canada as defined in the Seismic Hazard maps of 4$^{th}$, 5$^{th}$ and 6$^{th}$ generation (Adams and Halchuk 2003, Adams et al. 2015, Adams et al. 2019) lead to the necessity to better understand the seismic demand in practice. Given the historical low seismic concern in Eastern Canada, nonlinear analyses are still seldomly used, whereas extensive research and development of new models were done in Western Canada.

This study presents nonlinear ground response analyses performed on 33 sites in Quebec, using seismic records compatible with Eastern Seismic Hazard and scaled for an arbitrary target response spectrum defined as the uniform hazard spectrum in Montréal. From these analyses, soil seismic amplification factors were computed and compared to those featured in NBCC 2015. In practice, the results of the ground response analyses would be averaged and compared to the uniform hazard design spectrum (UHS) modified with the empirical site factors. This approach is not followed here, and this paper does not intend to reproduce what an engineer would do, but solely to study the accuracy of the amplification factors as compared to the results of ground response analyses. This paper shows that although the NBCC 2015 factors are often conservative, there is sometimes an underprediction of the amplification at the site natural period, which can lead to unsafe designs.

## 2. SOIL PROFILES CONSIDERED

### 2.1 Shear wave velocity profiles

33 soft soil sites were included in the study, derived from SCPT soundings performed in Québec. Of the 33 sites, 16 are considered class E and 17 class D, and the average $V_{S30}$ across all sites is 164 m/s.

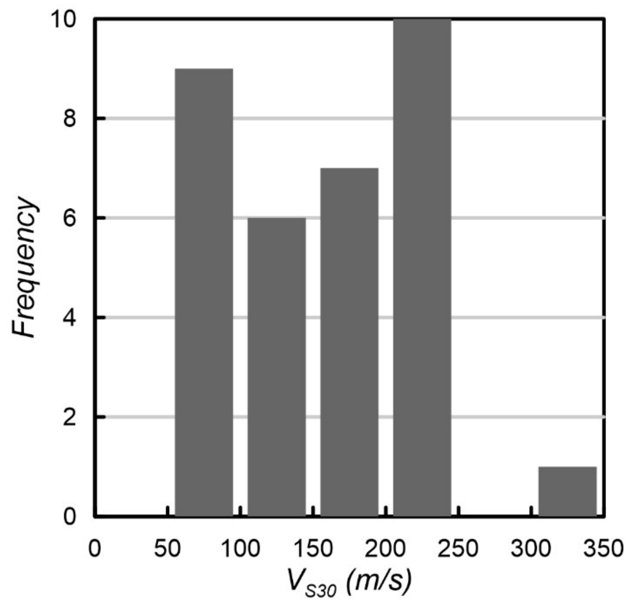


Figure 1. Distribution of $V_{S30}$ for the sites considered.

### 2.2 Soil properties

To perform ground response analysis on a large number of soil profiles, a procedure is established to segment the soil profiles into homogeneous layers and define all the necessary soil properties based on CPT data and shear wave velocity profiles.

The first step is to compute the soil index $I_c$ as defined in Robertson (1990) based on the normalized cone resistance and friction ratios, which can then be used to determine the soil type, clayey soils having $I_c$>2.6 and sandy soils $I_c$<2.6. For the sake of brevity, equations are not repeated here but can be found in Robertson and Cabal (2015). Because of the uncertainty and the inherent variability of the CPT test, values of $I_c$ fluctuates with depth (Figure 2). Using a fixed limit for $I_c$, such as 2.6 to separate between clay and sand layers, can generate a large number of soil segments. A soil segment is defined as a set of continuous sublayers. A large number of soil segments was often deemed unrealistic when comparing the soil segmentation to the boring logs, and it was decided to adjust the $I_c$ limit locally. Although debatable for varved clays sometimes found in Québec, and that contain interlayers of sands, this simplification was necessary due to the lack of knowledge of the seismic behavior of such soil deposits. When evaluating the entire soil profile, a new soil segment is detected when a soil layer's $I_c$ switches from a value lower than a limit value $I_{c,limit}$ to a higher value, or vice versa. $I_{c,limit}$ is initially set to 2.6 and then modified iteratively over different depth intervals. If over an interval of depth, a change of the threshold criterion from 2.6 to another value between 2.6 and 2.4 decreases the total number of sand and clay segments of a profile, as shown in Figure 2, the threshold criterion is then adjusted. This process is then repeated to minimize the total number of soil type changes. This produces a more realistic representation of the soil composition. For instance, in Figure 2, at depth between 5 and 8.3 m, using an $I_{c,limit}$ of 2.6 would segment this clay layer in 8 segments, while boreholes have confirmed that this is a homogeneous layer of clay.

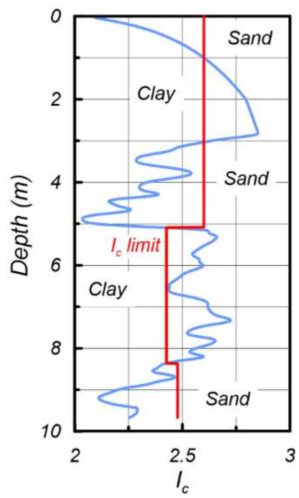


Figure 2. Example of segmentation based on the distribution of $I_c$ with depth.

The unit weight ($\gamma$) of each soil layer is calculated using the empirical relationship from Robertson (2010), while the shear strength ($S_u$) of the clayey layers is computed using the following equation (Robertson and Cabal 2015):

$$S_u = \frac{q_t - \sigma_v}{N_{kt}}, \tag{1}$$

where $q_t$ is the corrected cone resistance, $\sigma_v$ the total stress, and $N_{kt}$ a dimensionless factor with an assigned value of 14. When available, the vane shear measurements of a site, corrected by Bjerrum (1973), are used to calibrate the $N_{kt}$. To do so, specific $N_{kt}$ values are computed at the location of each vane shear test, and an average value for each segment is then used to compute the calibrated shear strength for the entire clay segment, as shown in Figure 3.

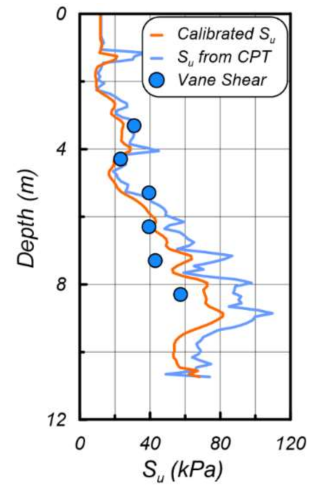


Figure 3. Calibration of $S_u$ when vane shear tests are available.

For the sandy layers, the shear strength ($\tau_{max}$) is calculated using Mohr-Coulomb:

$$\tau_{max} = \sigma'_{v0} \cdot \tan\varphi', \tag{2}$$

where $\sigma'_{v0}$ is the initial effective stress and $\varphi'$ is the friction angle calculated according to Robertson and Campanella (1983):

$$\tan(\varphi') = \frac{1}{2.68} * [log \frac{q_c}{\sigma'_{v0}} + 0.29]. \tag{3}$$

where $q_c$ is the measured cone resistance. The shear wave velocities ($V_s$) for clayey layers and sandy layers are calculated using the following correlations from Robertson and Cabal (2015) and Perret (2016) respectively:

$$V_s = \frac{\left[10^{(0.55I_c+1.68)} * \frac{q_t - \sigma_v}{p_a}\right]^{0.5}}{\left(\frac{p_a}{\sigma'_{v0}}\right)^{0.25}} \qquad \text{(clay)} \tag{4}$$

$$V_s = 28.27 * q_t^{0.137} * f_s^{0.013} * \sigma'_{v0}{}^{0.17} \qquad \text{(sand)} \tag{5}$$

Of the 33 sites considered, 11 had discrete field $V_S$ measurements available from seismic CPT. For these sites, the relationships are adjusted by a scaling factor so that the values computed match the field measurement. An example of initial $V_s$ estimations and their corresponding calibrations are shown in Figure 4. Note that this figure presents the profile with the most significant difference between Cabal's relationship and the field measurements. In other profiles, the difference was more subtle, although Cabal's relationship tended to slightly underpredict the shear wave velocity for the selected profiles. The scaling factor in any segment is computed to minimize the discrepancy between the measurement and the estimation within the soil segment. Soil segments without any field $V_s$ at a site, but with field $V_s$ measurement in other segments re-assigned a linearly interpolated scaling factor from neighbouring segments, except at the extremities where the closest scaling factor in a segment with field $V_s$ is used as a constant scaling. At the surface, a minimum value of 50 m/s is assigned for the shear wave velocity.

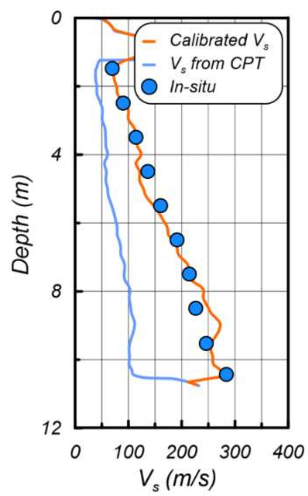


Figure 4. Calibration of $V_s$ when measurements are available

Based on the available data, it is impossible to accurately estimate the plasticity index (*PI*); therefore, for this study, a *PI* value of 30 is assigned to clay layers and a *PI* of 0 is assigned to sand layers. Although debatable, these values are deemed reasonable for the purpose of the study. Finally, the over-consolidation ratios of clayey layers (*OCR*) are calculated according to Kulhawy and Mayne (1990):

$$\mathrm{OCR} = 0.33 * \frac{(q_t - \sigma_{v0})}{\sigma'_{v0}} \qquad [6]$$

# 3. METHODOLOGY

## 3.1 Numerical modeling procedure

Total stress ground response analyses are performed using the software DEEPSOIL v.7.0 (Hashash et al. 2017). Simulations are ran using the nonlinear method and the ARCS model as formulated in Ynieta et al. (2017), and implemented in DEEPSOIL. Similarly to most 1D constitutive models for ground response analysis, the ARCS model requires a set of input modulus reduction and damping curves in order to define the stress-strain behavior of the soil. The model then uses a cubic spline and a coordinate transformation technique to match the input curves. Although the model can introduce small-strain hysteretic damping, the frequency independent damping formulation (Phillips and Hashash 2009) is used to introduce small strain damping.

Input modulus reduction and damping curves are defined for each layer with Darendeli's (2001) equations using the *PI*, the *OCR*, and the mean effective stress of the layer. The equations referred here are not shown in this paper for the sake of brevity. Note that modulus reduction curves defined from Darendeli's equations are only valid up to 0.3% of shear strain and are unable to represent the real shear strength of the soil. To solve this issue the modulus reduction curves are then adjusted for shear strength past a certain transition strain value ($\gamma_1$) according to Yee et al. (2013).

The soil profile is divided into sublayers which maximum thickness ($\Delta H$) is determined by the minimum $V_s$ in order to ensure that the frequency content of the motion is adequately propagated in the soil. Lysmer's criterion (Kuhlemeyer and Lysmer 1973) was retained to prevent artificial damping. The maximum thickness is calculated as followed:

$$\Delta \mathrm{H} < \frac{\mathrm{V_{s,minimum}/f}}{10}, \qquad [7]$$

where *f* is the maximum propagable frequency set to 50 Hz.

Finally, the bedrock is defined with a shear wave velocity ($V_s$) of 1600m/s, a unit weight ($\gamma$) of 25kN/m$^3$ and a damping ratio of 2% to represent potential bedrock found in Quebec.

## 3.2 Selection of Input Seismic Motions

22 input seismic motions are selected in this study from the NGA-West2 database (Ancheta et al. 2014), to be consistent with the seismic hazard in Montréal. The use of a database associated with a different seismicity was motivated by the lack of recordings available in stable continental region. In this study, only the seismic scenario controlling the seismic hazard at short periods (between 0.01 and 0.2 s) is considered. Other scenarios will be considered in future work. The seismic scenario is selected via deaggregation, a process which divides the seismic hazard into its different contributions and allows to define realistic seismic scenarios based on distance and magnitude. In this study, all 22 input seismic motions are selected in the following scenario:

i. a magnitude between 5 and 6,
ii. recorded on bedrock within 20km of the source of the earthquake,
iii. any scaling factor used to adjust the recording to the target spectrum over the range of periods of interest must be higher than 0.5 but lower than 2,
iv. the average input motion must be greater than 90% of target spectrum within the designated period interval of 0.01s to 0.2s.

Table 1 shows the selected input seismic motions used in this study.

Table 1. Input Seismic Motions Used in this Study

| Record Sequence Number | Name of Seismic Event | Magnitude | Recording Station |
|---|---|---|---|
| **98 Horizontal 1** | Hollister-03, USA | 5.14 | Gilroy Array #1 |
| **98 Horizontal 2** | Hollister-03, USA | 5.14 | Gilroy Array #1 |
| **156 Horizontal 1** | Norcia, Italy | 5.90 | Cascia |
| **156 Horizontal 2** | Norcia, Italy | 5.90 | Cascia |
| **381 Horizontal 1** | Coalinga-02, USA | 5.09 | Oil Fields Fire Station |
| **381 Horizontal 2** | Coalinga-02, USA | 5.09 | Oil Fields Fire Station |
| **1642 Horizontal 1** | Sierra Madre, USA | 5.61 | Cogswell Dam - Right Abutment |
| **1642 Horizontal 2** | Sierra Madre, USA | 5.61 | Cogswell Dam - Right Abutment |
| **2019 Horizontal 1** | Gilroy, USA | 4.90 | Gilroy - Gavilan Coll. |
| **2019 Horizontal 2** | Gilroy, USA | 4.90 | Gilroy - Gavilan Coll. |
| **3553 Horizontal 1** | Fruili-03, Italy | 5.50 | Tarcento |
| **3553 Horizontal 2** | Fruili-03, Italy | 5.50 | Tarcento |
| **3768 Horizontal 1** | Northridge-06, USA | 5.28 | Tarzana – Club House |
| **3768 Horizontal 2** | Northridge-06, USA | 5.28 | Tarzana – Club House |
| **4369 Horizontal 1** | Umbria Marche (aftershock 1), Italy | 5.5 | Nocera Umbra |
| **4369 Horizontal 2** | Umbria Marche (aftershock 1), Italy | 5.5 | Nocera Umbra |
| **4377 Horizontal 1** | Umbria Marche (aftershock 8), Italy | 5.2 | Borgo-Cerreto Torre |
| **4377 Horizontal 2** | Umbria Marche (aftershock 8), Italy | 5.2 | Borgo-Cerreto Torre |
| **8169 Horizontal 1** | San Juan Bautista, USA | 5.17 | San Andreas Geophysical Obs. |
| **8169 Horizontal 2** | San Juan Bautista, USA | 5.17 | San Andreas Geophysical Obs. |
| **8571 Horizontal 1** | El Mayor-Cucapah, Mexico | 7.20 | Padua |
| **8571 Horizontal 2** | El Mayor-Cucapah, Mexico | 7.20 | Padua |

## 4 RESULTS AND DISCUSSION

In this project, seismic nonlinear ground response analyses (GRA) were performed on 33 sites situated in Eastern Canada. For each of the 22 input motions at every site, the seismic amplification factors (AF) from the nonlinear analyses are obtained as follows at 113 spectral periods distributed between 0.01 and 10 s:

$$\text{Amplification factors (AF)} = \frac{\text{spectral response at the surface}}{\text{spectral response of the seismic input motion}} \qquad [8]$$

where the spectral response at the surface and of the seismic input motion are provided in the DEEPSOIL analyses results.

The average period-dependent amplification factors from the 22 input motions from the GRA at every site are then compared to the amplification factors provided in the NBCC 2015. More information on how these factors are interpreted are found in the guidelines provided by the NBCC 2015. Equivalent linear analyses were also performed, but the results are not presented herein. Although the results of EL analyses differed slightly from NL analyses, their trends, with respect to the factors from the code, were comparable.

Analyzing the estimated factors from ground response analyses and provided by the NBCC 2015, three main cases are observed and presented in figure 5, 6, 7 and 8. The distribution of cases is described subsequently. Note that in all figures, dash lines indicate plus and minus one standard deviation ($\sigma$) from the mean. Site factors from the code were computed for each individual motion, unlike the common practice of computing a unique set of factors for a single UHS, in order to present a fair comparison with the amplification of individual motions with varying PGA. This explains the variability in the site factors from the code.

Upon visual inspection, for 19 of the 33 sites, the site factors from GRA show a peak typically located around the natural site period ($T_0$) that is underpredicted by the NBCC 2015 factors (cases 1.a and 1.b). The natural site period is computed based on the modal decomposition of the $V_s$ profile and corresponds to the first fundamental mode of the system.

At the site shown in case 1.a (Figure 5), it is observable that at the natural site period, the amplification factors derived from the GRA are more than twice as much as the factors predicted by the NBCC 2015. For periods lower than the natural site period, the GRA still produce amplification factors significantly greater than those from the NBCC 2015. As for the rest of the periods, the NBCC 2015 seems to be conservative. Similarly, case 1.b (Figure 6) shows another site where the amplification factors derived from the GRA are significantly higher than the factors from the NBCC 2015 at the natural site period, even though the NBCC 2015 and the nonlinear analysis predicted similar factors for periods further away from the natural site period. Both case 1.a and 1.b show that the NBCC 2015 is not always conservative in designing against seismic hazards particularly around the natural site period.

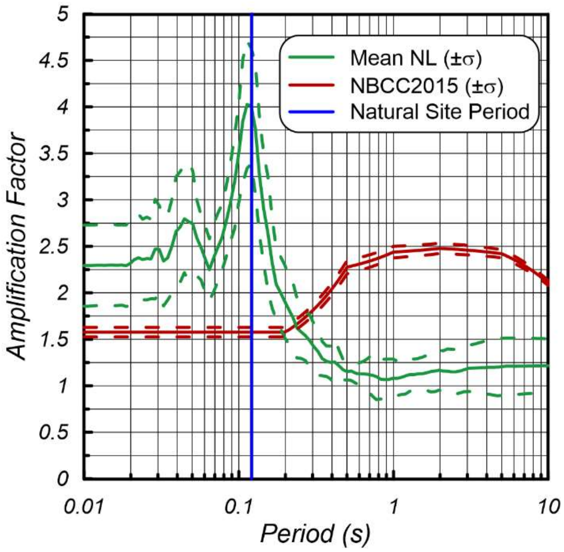


Figure 5. Comparison of amplification factors between nonlinear analysis and NBCC 2015 – case 1.a

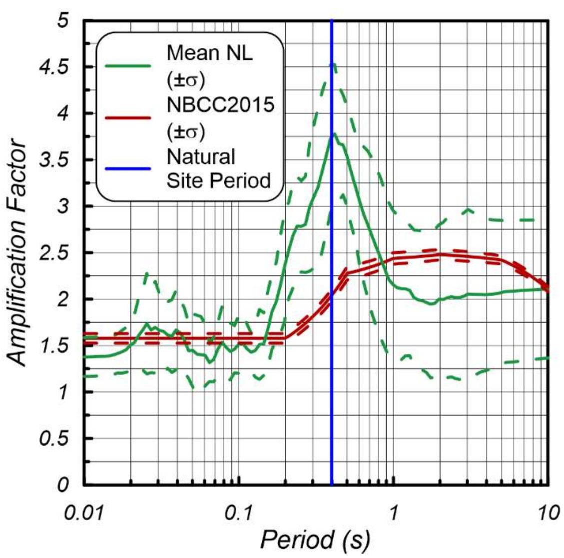


Figure 6. Comparison of amplification factors between nonlinear analysis and NBCC 2015 – case 1.b

At the site shown in case 2 (Figure 7), the NBCC 2015 is highly conservative when compared to nonlinear analyses, as they can at times provide amplification factors four times higher than those from nonlinear analyses. 5 of the 33 sites present such behavior, with all of them characterized as sites E, and among the softest. However, it is interesting to note that some of the softest sites fell under case 1, further indicating the complexity of site response. It is observable that in examples such as case 2, the peak of the amplification factors from the nonlinear analyses are located at periods slightly higher than the natural period of the site. A potential explanation for this is that under soil nonlinearity induced by strong ground motion, the stiffness of the soil reduces, and the site period lengthens. It is thus important to remember that the natural site period computed based on the $V_s$ profile is an elastic parameter.

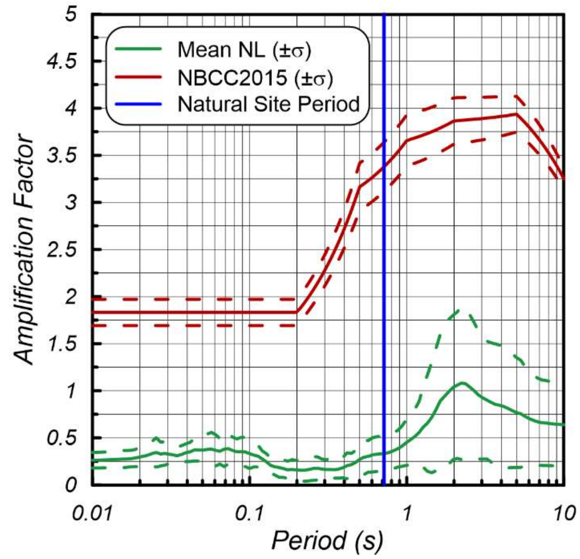


Figure 7. Comparison of amplification factors between nonlinear analysis and NBCC 2015 – case 2

In the third case, for 9 of the 33 sites presented, the averaged amplification factors from the NBCC 2015 were only slightly higher than the averaged factors predicted by the nonlinear analysis (Figure 8). Thus, the NBCC 2015 can occasionally agree fairly well with the results of GRA without being overly conservative. However, as observed from the standard deviation ($\sigma$) of the nonlinear analysis, some earthquakes can still cause amplifications factors higher than those from the NBCC 2015, despite the favourable overall average. In addition, it should be noted that for case 3, the peak amplification factor is also found around the natural site period.

Figure 9 presents the residual of the amplification factors (AF) for all motions at all sites computed as follows:

$$\text{Residual} = \ln\left(\frac{AF\ from\ GRA}{AF\ from\ the\ code}\right) \quad [9]$$

The results show an overall trend of conservatism, especially at long periods, but also a significant underprediction at some periods for about 25% of the motions. It should be noted that all these residuals are overall large, and denote a poor match between the ground response analysis and the code factors, much greater than the residuals observed when comparing GRA and measured site response in seismic event (e.g. Kaklamanos et al. 2015).

In Figure 10, the same residuals are plotted against the period normalized by the site period. The results show a clear peak at the site period (i.e. a normalized period of 1), indicating that at the site period, the code underpredicts the amplification.

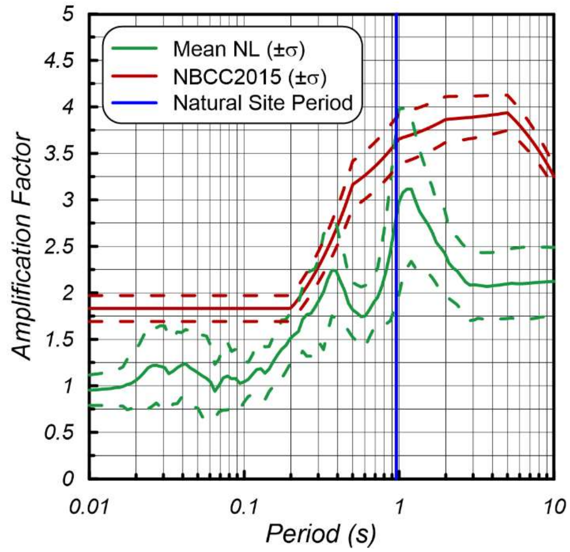

Figure 8. Comparison of amplification factors between nonlinear analysis and NBCC 2015 – case 3

In summary, according to this study, the NBCC 2015 can occasionally predict seismic amplification factors well. However, most of the results in this study suggests that the NBCC 2015 often produces conservative amplification factors, except at the site period. It should be noted that the apparent conservatism of the NBCC 2015 at long period might account for multidimensional long period effects not accounted for in a 1D ground response analysis, such as basin effects.

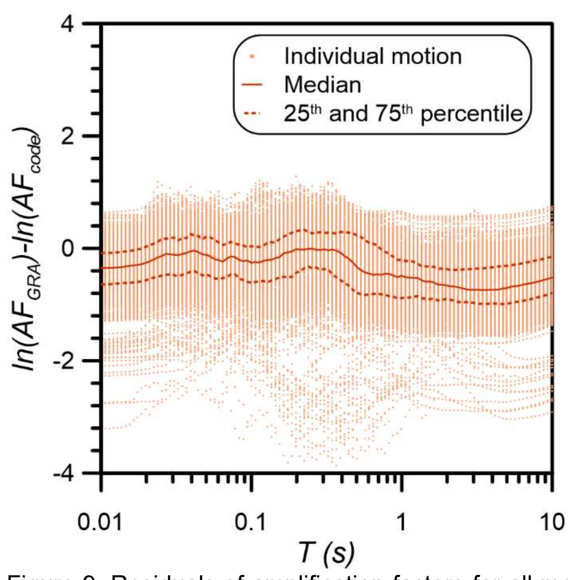

Figure 9. Residuals of amplification factors for all motions and all sites

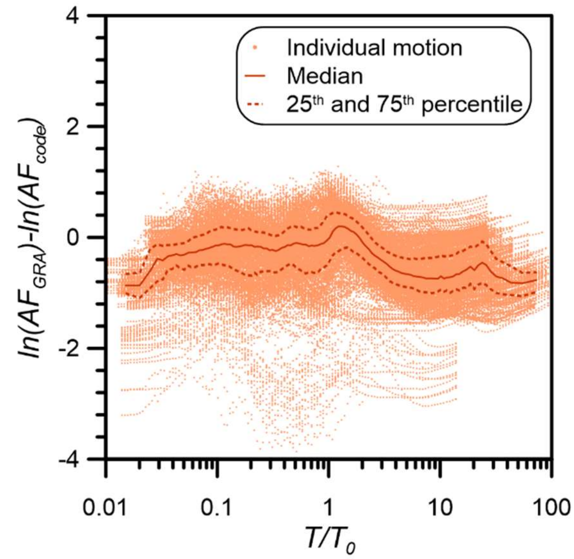

Figure 10. Residuals of amplification factors for all motions and all sites vs. normalized period

## 5 CONCLUSION

Among current established industry practices, the most commonly used method of determining seismic hazard due to amplification of seismic waves in soft soil deposits is to use the NBCC 2015 amplification factors. However, site-specific evaluation of potential for amplification is recommended. In this study, 22 input seismic motions were used on 33 sites located in Quebec to evaluate soil amplification of seismic waves via the more robust nonlinear seismic wave propagation method in order to compare the use of a more advanced method with the NBCC 2015 approach.

According to the results in this study, the NBCC 2015 can at times overestimate the amplification factors significantly, and lead to unnecessary costly design. However, the NBCC 2015 can sometimes significantly underestimate the amplification factors, particularly at the natural site period, causing potential risks to engineering designs in the event of an earthquake. Currently, the NBCC 2015 approach does not consider the natural site period when designing against seismic hazard amplification through soft soil deposits. However, as seen in this study, it could be beneficial to consider the effect of the natural site period on the amplification of seismic waves in soft soil deposits.

Future work includes further analysis of the residuals and exploring tendency in the results with regard to bias based on PGA, $V_{S30}$, and site natural period, for the motions presented herein, but also for supplemental motions and seismic scenarios. In particular, motions recorded in Eastern North America will be included.


## 6 ACKNOWLEDGEMENTS

The authors gratefully acknowledge the support and contributions of WSP. The authors would especially like to thank Morteza Esfehani and Benoit Latapie. Any opinions,

findings, conclusions, or recommendations expressed in this material are those of the author(s) and do not necessarily reflect the views of the company.

## 7 REFERENCES


Adams, J., and Halchuk, S. 2003. Fourth generation seismic hazard maps of Canada: Values for over 650 Canadian localities intended for the 2005 National Building Code of Canada. *Geological Survey of Canada Open File* 4459. 155 p.

Adams, J., Halchuk, S., Allen, T., & Rogers, G. 2015. Canada's 5th generation seismic hazard model, as prepared for the 2015 National Building Code of Canada. In *11th Canadian Conference on Earthquake Engineering* (pp. 21-24).

Adams, J., Allen, T., Halchuk, S., & Kolaj, M. 2019. Canada's 6th Generation Seismic Hazard Model, as Prepared for the 2020 National Building Code of Canada. 12th Can. Conf. *Earthquake Engineering*.

Ancheta, T. D., Darragh, R. B., Stewart, J. P., Seyhan, E., Silva, W. J., Chiou, B. S. J., ... & Kishida, T. 2014. NGA-West2 database. *Earthquake Spectra*, 30(3), 989-1005.

Bjerrum L. 1973. Problems of soil mechanics and construction on soft clays. Proc. 8th *Int. Conf. on Soil Mech. and Foundation Engineering*, Vol. 3, Moscow, 111–159.

Borcherdt, R. D. 1994. Estimates of site-dependent response spectra for design (methodology and justification). *Earthquake spectra*, 10, 617-617.

Buech, F., Davies, T. R., & Pettinga, J. R. 2010. The Little Red Hill Seismic Experimental Study: Topographic Effects on Ground Motion at a Bedrock-Dominated Mountain Edifice Little Red Hill Seismic Experimental Study: Topographic Effects on Ground Motion. *Bulletin of the Seismological Society of America*, 100(5A), 2219-2229.

Code, C. C. H. B. D. 2006. CAN/CSA S6-06. *Canadian Standards Association, Canada*, *734*.

Darendeli, M. B. 2001. Development of a new family of normalized modulus reduction and material damping curves. Ph.D. dissertation, University of Texas at Austin, Austin, Tex.

Finn, W. L., & Wightman, A. 2003. Ground motion amplification factors for the proposed 2005 edition of the National Building Code of Canada. *Canadian Journal of Civil Engineering*, 30(2), 272-278.

Groholski, D. R., Hashash, Y. M., Kim, B., Musgrove, M., Harmon, J., & Stewart, J. P. 2016. Simplified model for small-strain nonlinearity and strength in 1D seismic site response analysis. *Journal of Geotechnical and Geoenvironmental Engineering*, 142(9), 04016042.

Hashash, Y.M.A., Musgrove, M.I., Harmon, J.A., Ilhan, O., Groholski, D.R., Phillips, C.A., and Park, D. 2017. "*DEEPSOIL 7.0, User Manual*". University of Illinois at Urbana-Champaign, Urbana, Illinois.

Kaklamanos, J., Baise, L. G., Thompson, E. M., & Dorfmann, L. 2015. Comparison of 1D linear, equivalent-linear, and nonlinear site response models at six KiK-net validation sites. *Soil Dynamics and Earthquake Engineering*, 69, 207-219.

Kuhlemeyer, R. L., & Lysmer, J. 1973. Finite element method accuracy for wave propagation problems. *Journal of Soil Mechanics & Foundations Div*, *99*(Tech Rpt).

Kulhawy, F. H., & Mayne, P. W. 1990. *Manual on estimating soil properties for foundation design (No. EPRI-EL-6800).* Electric Power Research Inst., Palo Alto, CA (USA); Cornell Univ., Ithaca, NY (USA). Geotechnical Engineering Group.

Matasovic, N. 1993. Seismic response of composite horizontally-layered soil deposits. Ph.D. thesis, Univ. of California, Los Angeles.

Park, D., & Hashash, Y. M. 2004. Soil damping formulation in nonlinear time domain site response analysis. *Journal of Earthquake Engineering*, 8(02), 249-274.

Perret, D., Charrois, E., & Bolduc, M. 2016. Shear Wave Velocity Estimation from Piezocone Test Data for Eastern Canada Sands (Quebec and Ontario)–Extended Version with Appendices. *Geological Survey of Canada*.

Phillips, C., & Hashash, Y. M. 2009. Damping formulation for nonlinear 1D site response analyses. *Soil Dynamics and Earthquake Engineering*, 29(7), 1143-1158.

Robertson, P. K. 2010. Soil behaviour type from the CPT: an update. In *2nd international symposium on cone penetration testing*, USA (pp. 9-11).

Robertson, P. K., & Cabal, K. L. 2015. *Guide to Cone Penetration Testing for Geotechnical Engineering*. 6th. Signal Hill: Gregg Drilling and Testing, Inc.

Robertson, P. K., & Campanella, R. G. 1983. Interpretation of cone penetration tests. Part I: Sand. *Canadian Geotechnical Journal*, 20(4), 718-733.

Robertson, P.K. 1990. Soil classification using the cone penetration test. *Canadian Geotechnical Journal*, 27(1):151-158.

Schnabel, P., Seed, H. B., & Lysmer, J. 1972. Modification of seismograph records for effects of local soil conditions. *Bulletin of the Seismological Society of America*, *62*(6), 1649-1664.

Seed, H. B., & Idriss, I. M. 1969. Influence of soil conditions on ground motions during earthquakes. *Journal of the Soil Mechanics and Foundations Division*, 95(1), 99-138.

Yee, E., Stewart, J. P., & Tokimatsu, K. 2013. Elastic and large-strain nonlinear seismic site response from analysis of vertical array recordings. *Journal of Geotechnical and Geoenvironmental Engineering*, 139(10), 1789-1801.

Yniesta, S., Brandenberg, S. J., & Shafiee, A. 2017. ARCS: A one dimensional nonlinear soil model for ground response analysis. *Soil Dynamics and Earthquake Engineering*, 102, 75-85.